European Journal of Medicinal Chemistry 45 (2010) 4458–4466

Contents lists available at ScienceDirect

European Journal of Medicinal Chemistry

journal homepage: http://www.elsevier.com/locate/ejmech

Original article

Inhibition of monoamine oxidase by indole and benzofuran derivatives

Louis H.A. Prins, Jacobus P. Petzer, Sarel F. Malan*

Pharmaceutical Chemistry, School of Pharmacy, North-West University, Private Bag X6001, Potchefstroom 2520, South Africa

ARTICLE INFO

Article history:
Received 10 March 2010
Received in revised form
8 June 2010
Accepted 3 July 2010
Available online 31 July 2010

Keywords:
Monoamine oxidase (MAO)
Indole derivatives
Benzofuran derivatives
Parkinson's disease (PD)
Molecular docking
LigandFit

ABSTRACT

Monoamine oxidase (MAO) is an important drug target for the treatment of neurological disorders. A series of indole and benzofuran derivatives were synthesised and evaluated as inhibitors of the two MAO isoforms, MAO-A and MAO-B. In general, the derivatives were found to be selective MAO-B inhibitors with K_i values in the nanoMolar (nM) to microMolar (μM) concentration range. The most potent MAO-B inhibitor, 3,4-dichloro-N-(2-methyl-1H-indol-5-yl)benzamide, exhibited a K_i value of 0.03 μM and was 99 fold more selective for the B isoform. We conclude that these indole and benzofuran derivatives are promising reversible MAO-B inhibitors with a possible role in the treatment of neurodegenerative diseases such as Parkinson's disease (PD).

1. Introduction

Parkinson's disease (PD) is a condition associated with the degeneration of the dopamine containing nigrostriatal neurons [1]. The resulting depletion of striatal dopamine is responsible for the characteristic PD symptoms such as bradykinesia (slowness of movement), rigidity (stiffness), hypokinesia (reduction in movement amplitude), akinesia (absence of normal unconscious movements) and other extrapyramidal effects. Since monoamine oxidase A and B (MAO-A and -B) are involved in the metabolic degradation of dopamine in the brain, inhibitors of these enzymes are considered useful for the treatment of PD [2].

The MAO isoform predominantly found in the human brain is MAO-B [3]. It has also been demonstrated that brain MAO-B activity, but not MAO-A activity, increases with aging [4]. As MAO-B appears to be located in glial cells [5], this may be due to gliosis associated with aging. Not only is MAO-B a major dopamine metabolising enzyme but it is also involved in the formation of free radicals and other potentially neurotoxic species. In the catalytic cycle of MAO-B, 1 mol of hydrogen peroxide (H_2O_2) and dopaldehyde is produced for every mole of dopamine metabolised [6]. Both these metabolic by-products are toxic and may contribute to the pathogenesis of PD [7]. Increased MAO-B levels have also been observed in plaque-associated astrocytes in the brains of Alzheimer's disease (AD) patients. This increase in MAO-B activity produces an elevation in hydroxyl radicals (•OH), which has been correlated with amyloid-β (Aβ) plaque formation. Hence, the therapeutic potential of selective reversible MAO-B inhibitors does not rely solely on their ability to increase the biological half-life of dopamine (symptomatic effects) but also on their ability to potentially slow PD progression (neuroprotective effects) and to inhibit Aβ plaque formation [4].

(*R*)-Deprenyl (selegiline) (**1**) (Fig. 1) was one of the first selective MAO-B inhibitors to be identified [8] and has since been shown to possess neuroprotective properties [9,10]. These properties may, in part, be dependent on the ability of (*R*)-deprenyl to inhibit the MAO-B catalysed formation of H_2O_2 and dopaldehyde in the brain [11]. In 1981 it was found that an *N*-demethylated aminoindan propargylamine derivative, AGN 1135, also was a potent and selective inhibitor of MAO-B [12]. Unlike (*R*)-deprenyl, this compound is not an amphetamine derivative and therefore did not present with amphetamine associated sympathomimetic side-effects. The *R*(+)-enantiomer of AGN 1135, now called rasagiline (**2**), is nearly three orders of a magnitude more potent than the *S* (−)-enantiomer in inhibiting MAO-B [13]. Rasagiline is considered useful as an adjuvant to levodopa for the treatment of PD, as this compound enhances dopamine levels in the primate brain following systemic administration of levodopa. Youdim and co-

* Corresponding author. School of Pharmacy, University of the Western Cape, Private Bag X17, Bellville 7535, South Africa. Tel.: +27 21 9593190; fax: +27 21 9591588.
E-mail address: sfmalan@uwc.ac.za (S.F. Malan).

0223-5234/$ – see front matter © 2010 Elsevier Masson SAS. All rights reserved.
doi:10.1016/j.ejmech.2010.07.005

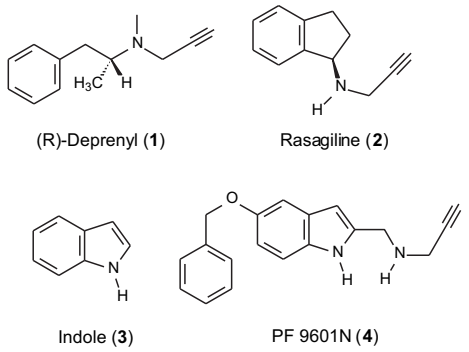

Fig. 1. Chemical structures of (*R*)-deprenyl (**1**), rasagiline (**2**), indole (**3**) and PF 9601N (**4**).

workers [14] showed that rasagiline also activates enzymes that play a key role in cellular events including mitochondrial viability, modulation of apoptotic processes and neuronal plasticity. These effects may further contribute to the observed protective effects of rasagiline.

Irreversible inhibition of MAO, however, have certain disadvantages including the fact that enzyme recovery requires the synthesis of new enzyme, the possible loss of selectivity as a result of repeated administration and an inhibition that is not affected by changes in substrate concentration [15]. The rate of enzyme biosynthesis, and hence recovery from irreversible inhibition is relatively slow and differs substantially between tissues and species. For example, a study by Fowler and co-workers [16] showed that the turnover rate for the synthesis of MAO-B in the human brain is close to 40 days. This was done by measuring the half-time for brain MAO-B synthesis in PD and in normal subjects after withdrawal from (*R*)-deprenyl. Reversible inhibition may be of a competitive, mixed, non-competitive or uncompetitive nature and possess the following advantages: the enzyme recovers as the inhibitor is eliminated from the tissues, the risk of loss of selectivity is far less because of a shorter duration of action and, in the case of competitive reversible inhibition, the inhibition is relieved when the substrate concentration is increased [15].

From the above discussion it is clear that the MAO-B inhibitors, (*R*)-deprenyl (**1**) and rasagiline (**2**), have an array of biological attributes that make them good candidates for the treatment and possible prevention of neurodegenerative disorders. Both of these are however irreversible MAO-B inhibitors, which is undesirable and current focus has shifted to the development of selective reversible MAO-B inhibitors [17–19].

Several previous studies [20–22] have indicated that the indole nucleus (**3**) may be useful as a scaffold for the design of MAO inhibitors. For example, a variety of indolylmethylamine derivatives have been shown to act as irreversible MAO inhibitors [23]. Of importance is the observation that bulky C5 substituents generally increase potency and selectivity for the MAO-B isoform. An example of such a substituent is the benzyloxy moiety (for example structure **4**) which is thought to enhance the selectivity towards MAO-B by increasing the molecular lipophilicity [24]. In the present study, we evaluated the possibility that the indole nucleus may be used in the design of reversible MAO inhibitors by synthesising a series of indole (**6a**–**d**) and structurally related benzofuran (**8a**–**d**) derivatives and evaluating them as inhibitors of recombinant human MAO-A and -B (Scheme 1). As shown in Scheme 1, the indole and benzofuran derivatives were substituted with a variety of C5 side chains. Based on the results of this study, a second series of indole derivatives (**6e**–**h**), which are structural analogues of compound **6b**, were synthesised and evaluated as MAO-A and -B inhibitors.

2. Results and discussion

2.1. Chemistry

The indole derivatives **6a**–**d**, **6f** and **6h** were synthesised by reacting 5-amino-2-methylindole (**5**) with the appropriate carboxylic acid in the presence of *N*-(3-dimethylaminopropyl)-*N*′-ethylcarbodiimide (EDC) as dehydrating agent [25–27]. For the synthesis of compounds **6e** and **6g** a similar procedure was followed, but in this instance *N*,*N*′-dicyclohexylcarbodiimide (DCC) was employed as dehydrating agent. The benzofuran derivatives (**8a**–**d**) were prepared according to the procedure reported by Scriven and co-workers [28] by reacting 5-hydroxy-3H-benzofuran-2-one (**7**) with the appropriate carboxylic acid in the presence of DCC to yield the esters (Scheme 1). The structures of the target compounds were confirmed by ^{1}H NMR, ^{13}C NMR, HRMS and IR while the purity was evaluated by HPLC analysis.

2.2. Enzyme inhibition studies

The MAO-A and -B activity measurements were based on the degree to which the MAO-A/B non-selective substrate, kynuramine (K_m = 16.1 μM and 22.67 μM for human recombinant MAO-A and -B, respectively), is oxidised by recombinant human MAO-A and -B to yield 4-hydroxyquinoline [29]. Kynuramine is non-fluorescent until undergoing oxidative deamination by MAO to produce the fluorescent metabolite 4-hydroxyquinoline (λ_{Ex} = 310 nm, λ_{Em} = 400 nm). Quantification of product formation was achieved by comparing the fluorescence emission of the samples to that of known amounts of authentic 4-hydroxyquinoline [29]. The IC_{50} values (concentration of the inhibitor that inhibits 50% of the enzyme activity) for the test compounds were determined by measuring the extent by which different concentrations of a test

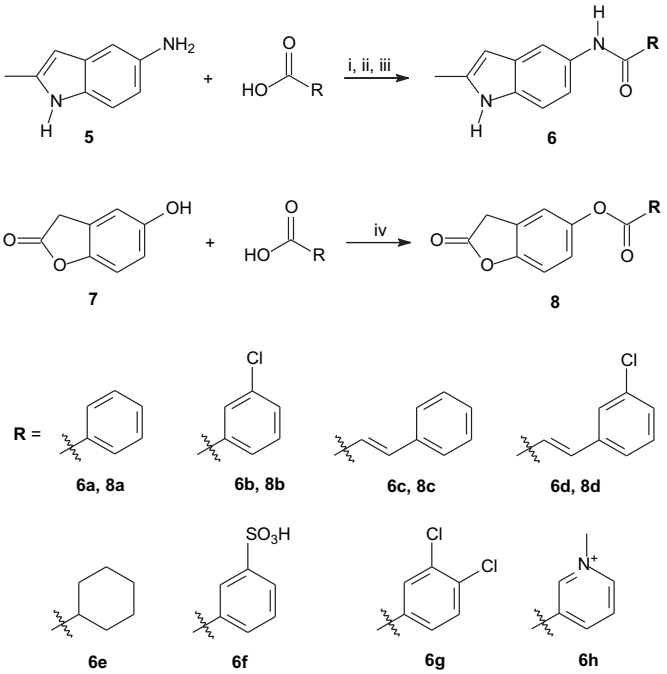

Scheme 1. Synthetic pathways to the indole (**6a**–**h**) and benzofuran (**8a**–**d**) derivatives: (i) EDC, dioxane/H_2O (**6a**–**d**); (ii) DCC, CH_2Cl_2 (**6e**, **6g**); (iii) EDC, MeOH (**6f**, **6h**) (iv) DCC, DMAP, CH_2Cl_2.

inhibitor slow the rate of the MAO catalysed deamination of kynuramine (Fig. 2). To allow for the calculation of the selectivity index (SI), the K_i values for the inhibition of MAO-A and -B were estimated from the experimentally determined IC_{50} values according to the Cheng–Prusoff equation [30].

The results of the MAO inhibition studies with compounds **6a**–**h** and **8a**–**d** are presented in Table 1. With the exception of **6d** and **8a** all of the derivatives were selective inhibitors of the MAO-B isozyme. Compound **8a** was essentially non-selective. Interestingly, chlorine substitution of the C5 phenyl side chain of the indoles and benzofuranes enhances both MAO-A and -B inhibition potencies since the unsubstituted homologues were less potent MAO inhibitors than the corresponding chlorine substituted compounds (for example compare **6b** with **6a**). The most potent MAO-B inhibitor was benzofuran **8d** with a K_i value of 0.19 μM. Compound **8d** was also the most potent MAO-A inhibitor of the test compounds. The most selective MAO-B inhibitor was indole **6b** with an SI of 25. Compound **6b** was also found to be a potent MAO-B inhibitor with a K_i value of 0.33 μM. Two other inhibitors, **8b** and **8c**, also exhibited MAO-B inhibition potencies in the sub-microMolar range. Compared to indole **6b**, the other potent MAO-B inhibitors of the series, benzofuranes **8b**–**d**, displayed relatively low selectivity for MAO-B (5–6 fold). Based on high inhibition potency and MAO-B selectivity as selection criteria, **6b** was considered a promising lead compound for the development of reversible MAO-B inhibitors.

In the second series, four structural derivatives (**6e**–**h**) of **6b** were synthesised and evaluated as inhibitors of recombinant human MAO-A and -B. The results of the MAO inhibition studies with compounds **6e**–**h** are presented in Table 1. Compound **6g** was found to be the most potent MAO-B inhibitor with a K_i value of 0.03 μM. Compound **6g** was also the most selective MAO-B inhibitor with an SI of 99. Since **6g** is the most potent and selective MAO-B inhibitor identified in this study, it can be concluded that the addition of an additional chlorine substituent to the phenyl ring at C5 of the indole ring is a suitable strategy to enhance binding affinity to the MAO-B active site. As mentioned above, chlorine substitution at the phenyl ring of the C5 side chain in general appears to enhance MAO-B inhibition activity of both the indoles and benzofuranes. By employing molecular docking studies, possible reasons for this observation are discussed in the next section. Interestingly, **6h** was found to inhibit MAO-A selectively (7 fold). This is in agreement with literature reports that positively charged structures, such as methylene blue, display affinity for the MAO-A active site [31,32]. The observation that **6e** is a relatively

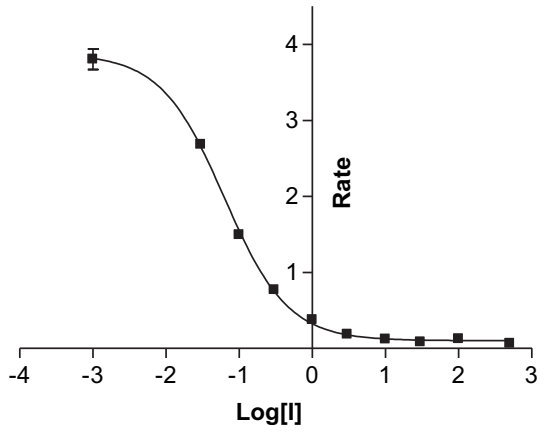

Fig. 2. Sigmoidal dose–response curve of the rate of MAO-B catalysed 4-hydroxyquinoline formation versus the logarithm of concentration of inhibitor **6g** (expressed in nM). Rates are expressed as nmol 4-hydroxyquinoline formed/mg protein/min. All determinations were performed in duplicate and are expressed as mean ± SEM.

Table 1
MAO inhibition by the indole (**6a**–**h**) and benzofuran (**8a**–**d**) derivatives.

Compound	MAO-A inhibition		MAO-B inhibition		SI[c]
	IC_{50} (μM)	K_i (μM)[a]	IC_{50} (μM)	K_i (μM)[b]	
6a	149.71 ± 4.10	39.45	3.84 ± 0.75	1.65	24
6b	31.04 ± 0.11	8.18	0.76 ± 0.17	0.33	25
6c	662.71 ± 65.27	174.63	18.82 ± 3.28	8.01	22
6d	7.67 ± 0.55	2.02	9.83 ± 1.63	4.23	0.5
6e	69.42 ± 2.01	18.29	6.96 ± 0.09	3.0	6
6f	259.07 ± 8.27	68.27	175.94 ± 11.51	75.72	0.9
6g	9.79 ± 1.26	2.58	0.06 ± 0.01	0.03	99
6h	20.76 ± 0.4	5.47	92.62 ± 1.87	39.86	0.1
8a	11.57 ± 0.32	3.05	8.89 ± 0.99	3.83	0.8
8b	7.66 ± 0.63	2.02	0.99 ± 0.1	0.43	5
8c	12.5 ± 0.18	3.29	1.2 ± 0.17	0.52	6
8d	3.9 ± 0.36	1.03	0.44 ± 0.03	0.19	5

[a] The experimentally determined IC_{50} values were used to calculate the K_i values according to the equation by Cheng and Prusoff: $K_i = IC_{50}/(1 + [S]/K_m)$ with $[S] = 45$ μM and K_m (Kynuramine) = 16.1 μM [30].
[b] The experimentally determined IC_{50} values were used to calculate the K_i values according to the equation by Cheng and Prusoff: $K_i = IC_{50}/(1 + [S]/K_m)$ with $[S] = 30$ μM and K_m (Kynuramine) = 22.67 μM [30].
[c] Relative selectivity for MAO-B is defined by the ratio of K_i(MAO-A)/K_i(MAO-B) for each compound.

weaker MAO-B inhibitor than **6a** indicates that phenyl substitution is more favourable for MAO-B inhibition than cyclohexyl substitution. Also, the weak inhibition of both MAO-A and -B by the sulfonyl substituted homologue **6f** supports the proposal that side chains with a relatively high degree of lipophilicity generally enhances affinity of inhibitors for the MAO-A and -B active sites [33,34].

2.3. Reversibility of inhibition

Another goal of the present study was to determine if the indole and benzofuran derivatives investigated here act as reversible or irreversible enzyme inhibitors. Since the most active derivatives are MAO-B inhibitors with only moderate to weak MAO-A inhibition potencies, the time-dependence of MAO-B inhibition was investigated with two potent derivatives, indole **6g** and benzofuran **8b**. Recombinant human MAO-B was pre-incubated with **6g** and **8b** for various periods of time (0–60 min). For this purpose the concentrations of the inhibitors were equal to 2 fold their respective IC_{50} values for the inhibition of MAO-B. The residual MAO-B activity was subsequently determined. As shown in Fig. 3, no time-dependent reduction in the rate of MAO-B catalysed oxidation of kynuramine is observed with both **6g** and **8b**. This indicated that the inhibition is reversible, at least for the time period (60 min) evaluated. Curiously, a marked increase of the MAO-B catalytic rate with increased preincubation time is observed for **8b**. One possible explanation for this observation is that **8b**, and probably the other benzofuran derivatives, is unstable in the potassium phosphate buffer used for the enzymatic reactions. The possibility exists that hydrolysis of the lactone and/or ester functional group may occur with the resulting loss of inhibition potential. Further studies are underway to investigate this observation.

To determine the mode of inhibition, sets of Lineweaver–Burk plots were constructed for the inhibition of MAO-B by **6g**. As shown in Fig. 4 the linear Lineweaver–Burk plots intersect on the *y*-axis for **6g**, which indicates that the mode of inhibition is competitive and therefore reversible.

2.4. Docking studies

While the indole and benzofuran derivatives investigated here were relatively weak MAO-A inhibitors, several derivatives were found to be potent inhibitors of MAO-B. Of these, compound **6g**,

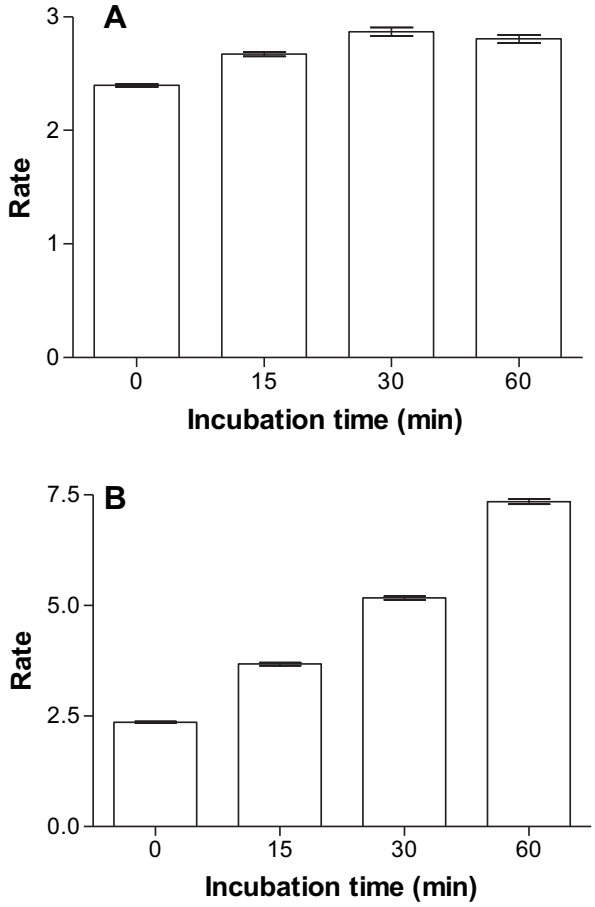

Fig. 3. The time-dependence of the inhibition of the recombinant human MAO-B by **6g** (panel A) and **8b** (panel B). MAO-B was pre-incubated for different periods of time (0–60 min) with the inhibitors and the initial rates (nmoles 4-hydroxyquinoline formed/min/mg protein) were recorded.

was the most potent and selective MAO-B inhibitor. To gain insight into the possible mode of binding of **6g** in the active site of MAO-B, molecular docking studies were performed. The most potent benzofuran derivative, **8d**, was also included in the docking study. For this purpose, the LigandFit application within Discovery Studio® 1.7 was used. The crystallographic structure of human recombinant MAO-B in complex with safinamide (PDB code: 2V5Z) [35], was selected as receptor model. The valences of the FAD co-factor and the co-crystallised ligand were corrected and the model was subjected to a three-step energy minimisation cascade while the protein backbone was constrained. Minimisation of the receptor proteins were considered necessary since the protein X-ray structure might contain residual energetic tensions from the crystallisation process. Following the energy minimisation cascade, the backbone constraint was removed and the co-crystallised ligand was deleted. With the exception of three highly conserved water molecules in the active site, all crystallographic waters were deleted from the protein model [35]. The structures of **6g** and **8d** were built, geometry optimised within Discovery Studio and docked into the protein model with LigandFit. Following the docking, the orientations and conformations of the docked ligands were further refined with the Smart Minimizer algorithm in Discovery Studio. Ten possible binding orientations were computed. To determine the accuracy of this docking protocol, the co-crystallised ligand, safinamide, was redocked into the MAO-B active site. This procedure was repeated three times and the best-ranked solutions of safinamide exhibited an RMSD value of 1.54 Å from the position of the co-crystallised ligand. Since RMSD values smaller than 2.0 Å generally indicate that the docking protocol is capable of accurately predicting the binding orientation of the co-crystallised ligand [36], this protocol was deemed to be suitable for the docking of inhibitors into the active site of MAO-B. The docking solutions were ranked according to their respective DockScore values.

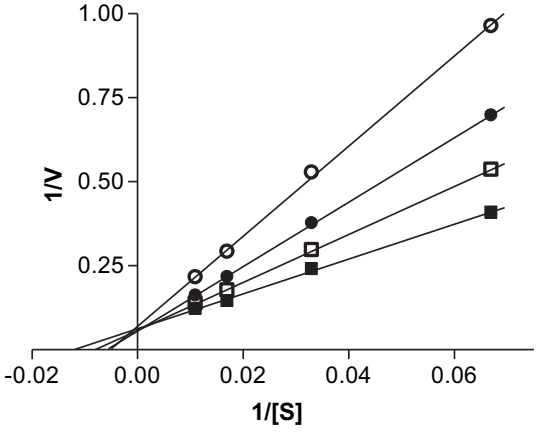

Fig. 4. Lineweaver-Burk plots of the inhibition of recombinant human MAO-B by **6g**. The lines were constructed in the absence (filled squares) and presence of 0.015 μM (open squares), 0.03 μM (filled circles) and 0.06 μM (open circles) of **6g**. The rate (V) is expressed as nmol 4-hydroxyquinoline formed/min/mg protein.

Examination of the best-ranked docking solution for **6g**, reveals that the relatively polar indole nucleus is located in the substrate cavity, in the vicinity of the FAD co-factor, with the C5 side chain extending towards the entrance cavity space of MAO-B (Fig. 5a). This binding orientation is similar to that observed for the co-crystallised ligand, safinamide, which also traverses both active site cavities [35]. The polar propanamidyl moiety of safinamide is also located in the substrate cavity while the apolar 3-fluorobenzyloxy side chain is stabilised within the entrance cavity space. As shown in Fig. 5a, the 3,4-dichlorophenyl moiety of **6g** is possibly stabilised by Van der Waals interactions in the hydrophobic entrance cavity defined by Phe-103, Trp-119, Leu-164, Leu-167, Phe-168 and Ile-316 [29]. Since the addition of chlorine would enhance the lipophilicity of a phenyl ring, these interactions may explain the observation that chlorine substitution of the phenyl side chains of the indoles and benzofuranes enhances MAO-B inhibition potency. Of importance is the observation that the amide carbonyl oxygen of **6g** is stabilised by hydrogen bond interaction with the phenolic hydrogen of Tyr-326 [37]. In MAO-A, the residue that corresponds to Tyr-326 (in MAO-B) is Ile-335 [38]. The resulting absence of these stabilising interactions may, in part, explain the lower MAO-A inhibition potencies of this inhibitor. Other significant interactions which may stabilise the MAO-B–**6g** complex include a possible π–π interaction [38] between the indole ring and the amide functional group of the Gln-206 side chain with an interplane distance of approximately 3.5 Å and a possible hydrogen bonding between the amide carbonyl oxygen of **6g** and an active site water molecule.

The best-ranked docking solution obtained for **8d** in the MAO-B active site is similar to that observed for **6g**. The polar benzofuran ring binds within the substrate cavity where it is stabilised by hydrogen bonding between the lactam functional group of the inhibitor and the phenolic hydrogen of Tyr-435 and two active site water molecules (Fig. 5b). These are the principal interactions which stabilises the benzofuran derivatives in the MAO-B active site. The C5 side chain of **8d** extends towards the entrance cavity space of MAO-B where it is stabilised by hydrophobic interactions.

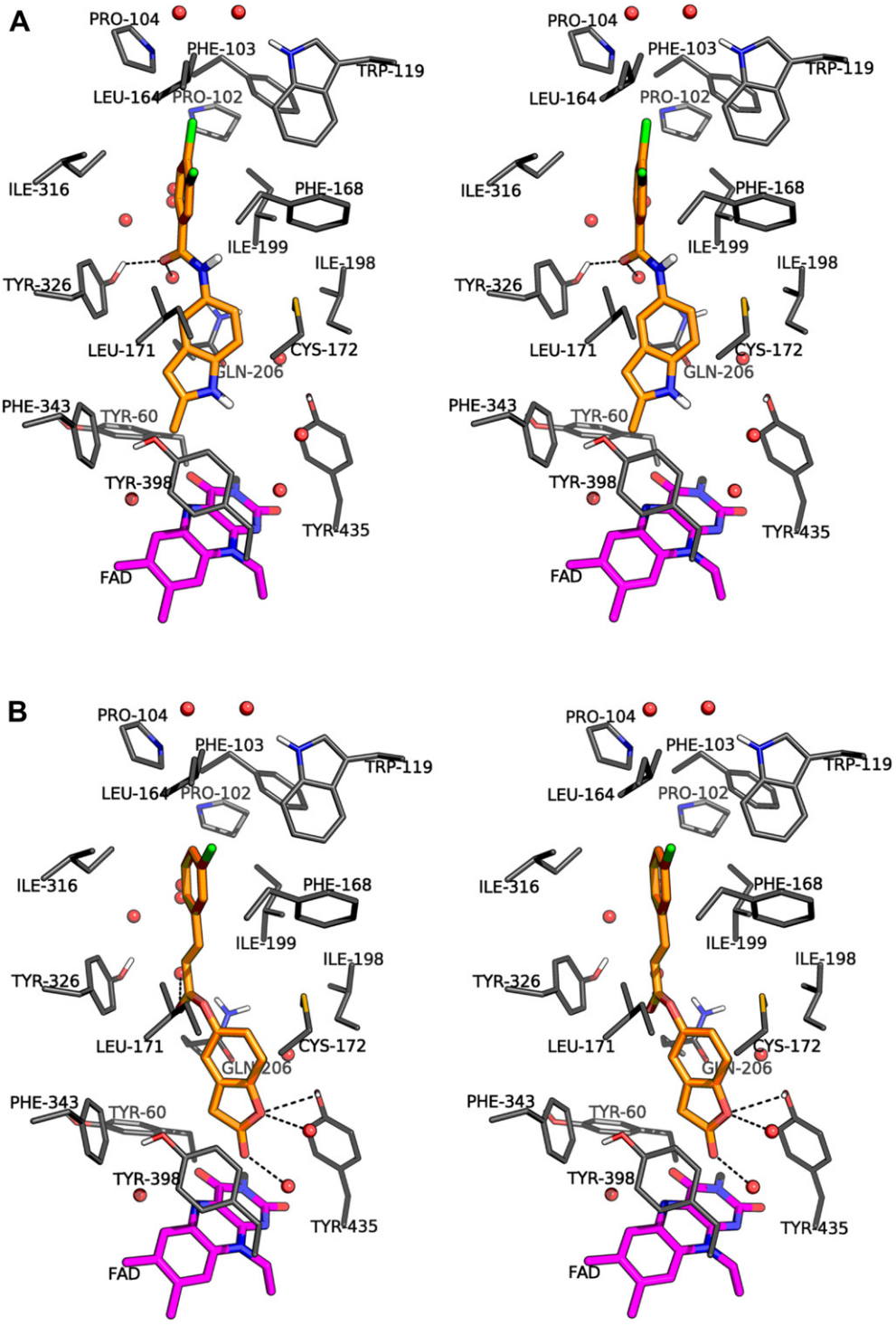

Fig. 5. Stereo view of the predicted binding modes of **6g** (Panel A) and **8d** (Panel B) in the human MAO-B active site. Hydrogens are hidden, except those involved in hydrogen bonds, and selected amino acid residues are displayed in grey. The FAD co-factor is displayed in magenta and hydrogen bonds shown as black dashes.

Similar to the analysis for **6g** above, the observation that chlorine substitution improves the MAO-B inhibition potencies of the benzofuranes (**8a**–**d**) may be due to enhancement of the lipophilicity of the C5 side chain. In contrast to the amide carbonyl of indole **6g**, the ester carbonyl oxygen of **8d** does not interact via hydrogen bonding with Tyr-326. The reason for this is that **8d** binds deeper (than **6g**) within the MAO-B active site in order to establish hydrogen bonding with the Tyr-435 and the two active site water molecules. It can therefore be concluded that hydrogen bonding with Tyr-326 is a major factor in stabilising the MAO-B–**6g** complex while polar interactions with Tyr-435 and the waters in the vicinity of the FAD co-factor are the major factors stabilising the MAO-B–**8d** complex. This analysis may explain why **8d** also exhibits affinity for the MAO-A active site. In MAO-A, the residue that corresponds to Tyr-435 (in MAO-B) is Tyr-444 [38]. Tyr-444 and water molecules present in the vicinity of the FAD co-factor may stabilise **8d** via hydrogen bonding in the MAO-A active site (Fig. 6), similar to that observed for the MAO-B active site. The proposal that benzofuran derivatives

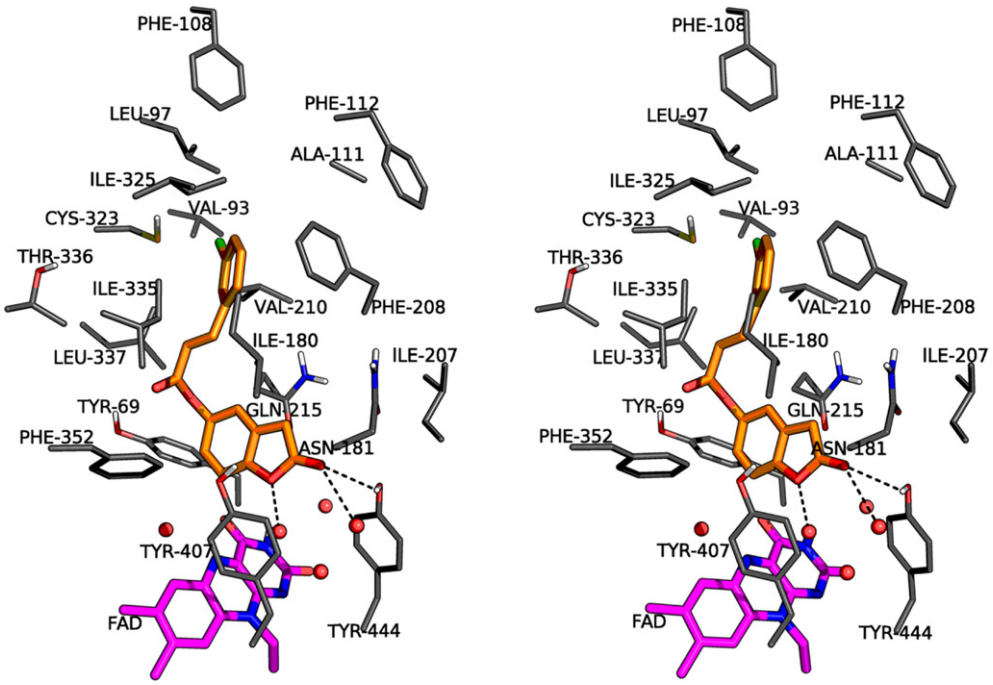

Fig. 6. Stereo view of the predicted binding mode of **8d** in the human MAO-A active site. Hydrogens are hidden, except those involved in hydrogen bonds, and selected amino acid residues are displayed in grey. The FAD co-factor is displayed in magenta and hydrogen bonds shown as black dashes.

are mainly stabilised by polar interactions in the substrate cavity may also explain the relatively small difference (~2 fold) in the MAO-B inhibition potencies of **8d** and its shorter side chain length homologue, **8b**. Regardless of the difference in chain lengths, both these homologues are expected to be stabilised to the same degree in the substrate cavity of MAO-B.

3. Conclusions

In the current study a series of indole and benzofuran derivatives were synthesised and evaluated as inhibitors of MAO-A and -B. In general, the derivatives were found to be selective for the MAO-B isoform with 3 benzofuranes and 2 indoles exhibiting inhibition potencies in the sub-microMolar range. Indole derivative **6g** was found to be the most potent and selective MAO-B inhibitor with a K_i value of 0.03 μM and a selectivity index of 99. As suggested by the molecular docking studies, the selective binding of **6g** to MAO-B may be explained by hydrogen bond interaction between the inhibitor and the phenolic hydrogen of Tyr-326. The corresponding residue in MAO-A, Ile-335 [38], would not undergo this interaction with **6g**. The most potent MAO-B inhibitor among the benzofuran derivatives was **8d** with a K_i value of 0.19 μM and a selectivity index of 5. Molecular docking suggests that **8d** is stabilised in the MAO-B active site principally by hydrogen bonding with Tyr-435 and the waters in the vicinity of the FAD co-factor. The suggestion that similar polar interactions are possible between **8d** and the active site of MAO-A may explain the relatively low isoform selectivity of this inhibitor.

An important observation is that chlorine substitution at the C5 phenyl side chain of the indoles and benzofuranes enhances both MAO-A and -B inhibition potencies. This may be due to the enhancement of nonspecific hydrophobic interactions between the inhibitors and the active sites of the MAO isozymes. Halogen substitution of an aromatic ring may therefore be considered as a general strategy to improve the binding affinities of ligands to MAO-A and -B. An important consideration however, is that the binding of these ligands should place the halogen in the hydrophobic pockets located towards the entrance of the active site cavities of the two enzymes.

We conclude that the benzofuran nucleus, in general, is a good scaffold for designing potent, relatively non-selective MAO inhibitors and that the indole nucleus show promise as scaffold for developing potent, MAO-B selective inhibitors.

4. Experimental

4.1. General methods

Thin-layer chromatography was performed on 0.20 mm thick aluminium silica gel sheets (Alugram® SIL G/UV254, Kieselgel 60, Macherey-Nagel® Düren, Germany) with an appropriate mobile phase and visualisation was achieved using UV light (254 and 366 nm) and iodine vapour. All melting points (mp) were obtained using a Stuart® Scientific SMP10 melting point apparatus and are uncorrected. ^{1}H and ^{13}C NMR spectra were recorded using a Bruker® Avance III 600 spectrometer at a frequency of 600 and 150 MHz, respectively. Chemical shifts are expressed in parts per million (δ) relative to the signal from tetramethylsilane (Me_4Si), added to the deuterated solvent DMSO-d_6. Spin multiplicities are given as s (singlet), d (doublet), dd (doublet of doublets) and m (multiplet). IR spectra were recorded in KBr on a Nicolet® Nexus™ 470-FT IR spectrometer over the range 400–4000 cm^{-1} employing the diffuse reflectance method. Direct insertion electron impact ionization (EIMS) and high resolution mass spectra (HRMS) were obtained on a DFS high resolution magnetic sector mass spectrometer (Thermo Electron Corporation).

HPLC analyses were performed using an Agilent® 1100 series HPLC equipped with a quaternary gradient pump, autosampler, diode array UV detector and Chemstation® data acquisition and analysis software. A Venusil XBP C18 column (4.60 × 150 mm, 5 μm) was used and elution was effected by means of a linear gradient starting at 30% acetonitrile to 85% acetonitrile after 5 min and holding at 85% acetonitrile until 10 min, where after the instrument was re-equilibrated at the starting conditions for 5 min. Standard solutions (1 mM)

of each of the eight test compounds were prepared in analytical grade acetonitrile and analysed at wavelengths of 210, 254 and 300 nm over a 15 min time period. The mobile phase flow rate was 1 mL/min and the injection volume was 20 μL.

4.2. Synthesis

4.2.1. General synthetic method for indoles **6a–d**

5-Amino-2-methylindole (500 mg, 3.42 mmol) and EDC hydrochloride (947 mg, 4.94 mmol) were dissolved in 20 mL dioxane/water (1:1). The appropriate benzoic acid or cinnamic acid (3.67 mmol) was added to the solution and the pH of the suspension adjusted to 5 with 2 M HCl (aq). The reaction mixture was stirred at room temperature for 2 h where after the pH was adjusted to 7 with 1 M NaOH (aq). Cooling the reaction with an external ice bath resulted in the final products (**6a–d**) precipitating from the reaction mixture. The precipitates were collected by filtration, giving the amide products in good yield, without the need for further purification [27].

4.2.2. N-(2-Methyl-1H-indol-5-yl)benzamide (**6a**)

The melting point of this compound corresponds to that described in literature (192–192.5 °C) [39]. Yield: 230 mg (27%); R_f = 0.47 (diethyl ether); mp: 190–193 °C ^{1}H NMR [600 MHz, DMSO-d_6]: δ = 10.90 (s, 1H), 10.09 (s, 1H), 8.00 (s, 1H), 7.88 (s, 1H), 7.64–7.52 (m, 3H), 7.39–7.21 (m, 3H), 6.12 (s, 1H), 2.42 ppm (s, 3H); ^{13}C NMR [150 MHz, DMSO-d_6]: δ = 164.0 (C), 137.0 (C), 136.0 (C), 134.0 (C), 131.6 (CH), 131.0 (C), 128.0 (3 × CH), 127.5 (C, CH), 115.0 (CH), 112.0 (CH), 110.0 (CH), 99.3 (CH), 13.5 ppm (CH_3); IR (KBr): ν_{max} = 3378, 3285, 2924, 2851, 1653, 1578, 1385, 912, 892, 856, 840, 797, 747, 713, 690 cm^{-1}. Compound purity (HPLC): 98.3%. EIMS *m*/*z* 250 (M$^{\bullet+}$); HRMS calcd. 250.1106, found 250.1102.

4.2.3. 3-Chloro-N-(2-methyl-1H-indol-5-yl)benzamide (**6b**)

Yield: 369 mg (38%); R_f = 0.62 (diethyl ether); mp: 178–182 °C ^{1}H NMR [600 MHz, DMSO-d_6]: δ = 10.86 (s, 1H), 10.13 (s, 1H), 8.01–8.00 (m, 1H), 7.94–7.90 (m, 1H), 7.82 (s, 1H), 7.66–7.61 (m, 1H), 7.58–7.52 (m, 1H), 7.32–7.26 (m, 1H), 7.24–7.19 (m, 1H), 6.10 (s, 1H), 2.36 ppm (s, 3H); ^{13}C NMR [150 MHz, DMSO-d_6]: δ = 163.5 (C), 137.5 (C), 136.3 (CH), 133.3 (CH), 133.2 (CH), 131.0 (C), 130.5 (C), 130.3 (C), 128.4 (C), 127.3 (C), 126.3 (CH), 114.9 (CH), 111.5 (CH), 110.1 (CH), 99.3 (CH), 13.5 ppm (CH_3); IR (KBr): ν_{max} = 3377, 3166, 2925, 2852, 1647, 1569, 1382, 913, 891, 869, 845, 799, 731, 675 cm^{-1}. Compound purity (HPLC): 98.6%. EIMS *m*/*z* 284 (M$^{\bullet+}$); HRMS calcd. 284.0716, found 284.0711.

4.2.4. (2E)-N-(2-Methyl-1H-indol-5-yl)-3-phenylprop-2-enamide (**6c**)

Yield: 859 mg (91%); R_f = 0.49 (diethyl ether); mp: 198–200 °C (decomp). ^{1}H NMR [600 MHz, DMSO-d_6]: δ = 10.88 (s, 1H), 10.02 (s, 1H), 7.90 (s, 1H), 7.70–7.60 (m, 2H), 7.57 (d, *J* = 15.63 Hz, 1H) 7.50–7.36 (m, 3H), 7.25 (dd, *J* = 7.85, 8.21 Hz, 2H), 6.91 ppm (d, *J* = 15.66 Hz, 1H); ^{13}C NMR [150 MHz, DMSO-d_6]: δ = 162.9 (C), 139.0 (CH), 136.3 (C), 134.2 (C), 133.0 (C), 131.1 (C), 129.5 (CH), 129.0 (CH), 128.9 (CH), 127.5 (C, 2 × CH), 123.0 (CH), 113.5 (CH), 110.3 (CH), 109.8 (CH), 99.2 (CH), 13.4 ppm (CH_3); IR (KBr): ν_{max} = 3423, 3288, 3052, 2854, 1651, 1592, 1450, 992, 894, 887, 866, 811, 799, 784, 775, 748 cm^{-1}. Compound purity (HPLC): 97.6%. EIMS *m*/*z* 276 (M$^{\bullet+}$); HRMS calcd. 276.1263, found 276.1259.

4.2.5. (2E)-3-(3-Chlorophenyl)-N-(2-methyl-1H-indol-5-yl)prop-2-enamide (**6d**)

Yield: 773 mg (73%); R_f = 0.51 (diethyl ether); mp: 155–160 °C ^{1}H NMR [600 MHz, DMSO-d_6]: δ = 10.86 (s, 1H), 10.00 (s, 1H), 7.90 (s, 1H), 7.70 (s, 1H), 7.63–7.57 (m, 1H), 7.54 (d, *J* = 16.03 Hz, 1H), 7.50–7.43 (m, 2H), 7.22 (s, 2H), 6.93 (d, *J* = 16.03 Hz, 1H), 6.10 (s, 1H), 2.37 ppm (s, 3H); ^{13}C NMR [150 MHz, DMSO-d_6]: δ = 163.0 (C), 137.8 (2 × CH), 136.8 (C), 134.2 (C), 133.5 (C), 131.5 (C), 131.3 (C), 129.6 (CH), 129.0 (CH), 127.7 (C), 126.5 (CH), 125.2 (CH), 114.0 (CH), 110.8 (CH), 110.3 (CH), 99.8 (CH), 13.9 ppm (CH_3); IR (KBr): ν_{max} = 3410, 3236, 3049, 2853, 1655, 1595, 1485, 997, 984, 912, 884, 859, 800, 783, 745, 687, 671 cm^{-1}. Compound purity (HPLC): 98.0%. EIMS *m*/*z* 310 (M$^{\bullet+}$); HRMS calcd. 310.0873, found 310.0866.

4.2.6. General synthetic method for indoles **6e–h**

Compounds **6e** and **6g**: The appropriate benzoic acid (4.1 mmol) was dissolved in 10 mL CH_2Cl_2 (anhydrous) where after DCC (932 mg, 4.52 mmol) was dissolved in an additional 10 mL CH_2Cl_2 (anhydrous) and added to the benzoic acid solution. The mixture was stirred on an external ice bath for 6 h and the *N*,*N*′-dicyclohexylurea (DCU) produced during activation of the carboxylic acid, was removed by filtration. 5-Amino-2-methylindole (600 mg, 4.1 mmol) was dissolved in 10 mL CH_2Cl_2 (anhydrous) and added to the reaction mixture. After allowing the reaction to stir at room temperature for 80 h, purification was performed with column chromatography using diethyl ether as mobile phase.

Compounds **6f** and **6h**: 5-Amino-2-methylindole (500 mg, 3.42 mmol) and the appropriate benzoic acid (3.49 mmol) were dissolved in 40 mL methanol. EDC hydrochloride (720 mg, 3.49 mmol) was added and the reaction allowed to stir at room temperature for 85 h. Compound **6h** was collected from the reaction mixture by filtration, without the need for further purification. Compound **6f** was purified by column chromatography with ethanol (anhydrous) as mobile phase [25].

4.2.7. N-(2-Methyl-1H-indol-5-yl)cyclohexanecarboxamide (**6e**)

Yield: 258 mg (25%); R_f = 0.66 (diethyl ether); mp: 198–200 °C ^{1}H NMR [600 MHz, DMSO-d_6]: δ = 10.74 (s, 1H), 9.49 (s, 1H), 7.70 (s, 1H), 7.11 (dd, *J* = 8.44, 8.54 Hz, 2H), 6.02 (s, 1H), 2.33 (s, 4H), 1.78–1.63 (m, 2H), 1.44–1.38 (m, 2H), 1.28–1.09 ppm (m, 6H); ^{13}C NMR [150 MHz, DMSO-d_6]: δ = 173.6 (C), 136.0 (C), 132.7 (C), 131.3 (C), 128.4 (C), 113.7 (CH), 110.0 (CH), 109.8 (CH), 99.1 (CH), 44.8 (CH), 29.3 (2 × CH_2), 25.3 (3 × CH_2), 13.4 ppm (CH_3); IR (KBr): ν_{max} = 3253, 3089, 2930, 2856, 1656, 1587, 1518, 1481, 1448, 897, 795, 770 cm^{-1}. Compound purity (HPLC): 97.7%. EIMS *m*/*z* 256 (M$^{\bullet+}$); HRMS calcd. 256.1576, found 256.1569.

4.2.8. 3-[(2-Methyl-1H-indol-5-yl)carbamoyl]benzene-1-sulfonic acid (**6f**)

Yield: 1 g (94%); R_f = 0.71 (ethanol); mp: 222–225 °C ^{1}H NMR [600 MHz, DMSO-d_6]: δ = 10.85 (s, 1H), 10.15 (s, 1H), 8.22 (s, 1H), 7.92 (d, *J* = 7.39 Hz, 1H), 7.84 (s, 1H), 7.79 (d, *J* = 7.39 Hz, 1H), 7.47 (t, 1H), 7.26 (dd, *J* = 9, 9 Hz, 2H), 6.09 (s, 1H), 2.36 (s, 3H), 1.05 ppm (t, 1H); ^{13}C NMR [150 MHz, DMSO-d_6]: δ = 164.8 (C), 148.3 (C), 136.2 (C), 135.1 (C), 133.2 (C), 130.8 (C), 128.4 (CH), 127.8 (CH), 127.6 (CH), 124.9 (C, CH), 115.0 (CH), 111.4 (CH), 110.1 (CH), 99.3 (CH), 13.5 ppm (CH_3); IR (KBr): ν_{max} = 3630, 3259, 3072, 2921, 1642, 1542, 1481, 1451, 1195, 1043, 917, 875, 803, 771, 752, 739, 676 cm^{-1}. Compound purity (HPLC): 91.2%.

4.2.9. 3,4-Dichloro-N-(2-methyl-1H-indol-5-yl)benzamide (**6g**)

Yield: 201 mg (15%); R_f = 0.74 (diethyl ether); mp: 200 °C ^{1}H NMR [600 MHz, DMSO-d_6]: δ = 10.88 (s, 1H), 10.19 (s, 1H), 8.21 (s, 1H), 7.86 (dd, *J* = 8.17, 8.15 Hz, 2H), 7.82 (s, 1H), 7.25 (dd, *J* = 8.57, 8.34 Hz, 2H), 6.10 (s, 1H), 2.36 ppm (s, 3H); ^{13}C NMR [150 MHz, DMSO-d_6]: δ = 162.6 (C), 136.4 (C), 135.8 (C), 133.9 (C), 133.4 (C), 131.2 (C), 130.7 (CH), 130.3 (C), 129.5 (CH), 128.4 (C), 127.9 (CH), 114.8 (CH), 111.5 (CH), 110.1 (CH), 99.3 (CH), 13.5 ppm (CH_3); IR (KBr): ν_{max} = 3304, 3090, 2922, 2854, 1928, 1855, 1824, 1794, 1741, 1707, 1632, 1587, 914, 873, 849, 836, 786, 762, 751, 680 cm^{-1}.

Compound purity (HPLC): 97.7%. EIMS *m/z* 318 ($M^{\bullet+}$); HRMS calcd. 318.0327, found 318.0315.

4.2.10. 1-Methyl-N-(2-methyl-1H-indol-5-yl)-1λ^4-pyridine-3-carboxamide (**6h**)

Yield: 410 mg (55%); R_f = not calculable; mp: 258–260 °C (decomp). ^{1}H NMR [600 MHz, DMSO-d_6]: δ = 11.05 (s, 1H), 10.86 (s, 1H), 9.81 (s, 1H), 9.12 (s, 2H), 8.22–8.19 (m, 1H), 7.91 (s, 1H), 7.35 (dd, J = 8.58, 8.57 Hz, 2H), 6.11 (s, 1H), 4.45 (s, 3H), 2.38 ppm (s, 3H); ^{13}C NMR [150 MHz, DMSO-d_6]: δ = 159.3 (C), 146.4 (CH), 145.3 (CH), 143.2 (CH), 136.3 (C), 134.1 (C), 133.4 (C), 129.7 (C), 128.2 (C), 126.8 (CH), 114.4 (CH), 111.2 (CH), 109.9 (CH), 99.0 (CH), 47.8 (CH_3), 13.0 ppm (CH_3); IR (KBr): ν_{max} = 3349, 3079, 2860, 1674, 1633, 1592, 1549, 1508, 1480, 1428, 1387, 904, 882, 856, 808, 745, 731, 693 cm^{-1}.

4.2.11. General synthetic method for benzofuranes **8a–d**

The appropriate benzoic acid or cinnamic acid (4.54 mmol) was dissolved in 10 mL CH_2Cl_2 (anhydrous) where after 4-dimethylaminopyridine (DMAP) (37 mg, 0.3 mmol) was added to the solution at room temperature. 5-Hydroxy-3H-benzofuran-2-one (500 mg, 3.33 mmol) was dissolved in 5 mL *N,N′*-dimethylformamide (DMF) (anhydrous) and added to the reaction mixture. The reaction was cooled with an external ice bath for 5 min. DCC (687 mg, 3.33 mmol) was dissolved in 5 mL CH_2Cl_2 (anhydrous) and added to the reaction while on ice. The reaction was stirred on ice for 5 min and the DCU produced during activation of the carboxylic acid, was removed by filtration. The external ice bath was removed and the reaction was stirred at room temperature for 24 h. The pure benzofuran derivatives (**8a–d**) were obtained through column chromatography with ethyl acetate/petroleum ether (1:1) as mobile phase [28].

4.2.12. Benzoic acid 2-oxo-2,3-dihydro-benzofuran-5-yl ester (**8a**)

Yield: 393 mg (46%); R_f = 0.71 (ethyl acetate/petroleum ether (1:1)); mp: 83–85 °C ^{1}H NMR [600 MHz, DMSO-d_6]: δ = 8.12–8.11 (m, 2H), 7.59–7.57 (m, 1H), 7.46–7.30 (m, 3H), 7.08 (s, 1H), 7.05 (s, 1H), 3.71 ppm (s, 2H); ^{13}C NMR [150 MHz, DMSO-d_6]: δ = 173.7 (C), 165.3 (C), 152.1 (C), 147.1 (C), 133.8 (CH), 130.7 (CH), 130.1 (CH), 129.1 (C), 128.6 (CH), 128.5 (CH), 124.0 (C), 122.2 (CH), 118.7 (CH), 111.4 (CH), 33.3 ppm (CH_2); IR (KBr): ν_{max} = 1805, 1738, 1479, 1264, 1138, 1120, 1052, 1023, 895, 875, 822, 809, 768, 713, 685, 669 cm^{-1}. Compound purity (HPLC): 96.4%. EIMS *m/z* 254 ($M^{\bullet+}$); HRMS calcd. 254.0579, found 254.0576.

4.2.13. 3-Chlorobenzoic acid 2-oxo-2,3-dihydro-benzofuran-5-yl ester (**8b**)

Yield: 563 mg (59%); R_f = 0.68 (ethyl acetate/petroleum ether (1:1)); mp: 90–93 °C ^{1}H NMR [600 MHz, DMSO-d_6]: δ = 8.14 (m, 1H), 8.05–8.04 (m, 1H), 7.61 (m, 1H), 7.41–7.39 (m, 1H), 7.16–7.10 (m, 3H), 3.77 ppm (s, 2H); ^{13}C NMR [150 MHz, DMSO-d_6]: δ = 173.6 (C), 164.1 (C), 152.3 (C), 146.9 (C), 134.8 (C), 133.8 (CH), 130.1 (C), 130.0 (CH), 129.8 (CH), 128.3 (CH), 124.1 (C), 122.1 (CH), 118.5 (CH), 111.4 (CH), 33.3 ppm (CH_2); IR (KBr): ν_{max} = 1801, 1734, 1480, 1249, 1136, 1106, 1073, 1053, 898, 877, 817, 780, 747, 708, 679, 660 cm^{-1}. Compound purity (HPLC): 97.4%. EIMS *m/z* 288 ($M^{\bullet+}$); HRMS calcd. 288.0189, found 288.0201.

4.2.14. (E)-Cinnamic acid 2-oxo-2,3-dihydro-benzofuran-5-yl ester (**8c**)

Yield: 470 mg (50%); R_f = 0.66 (ethyl acetate/petroleum ether (1:1)); mp: 75–80 °C ^{1}H NMR [600 MHz, DMSO-d_6]: δ = 7.75 (d, J = 15.97 Hz, 1H), 7.47–7.45 (m, 2H), 7.37–7.23 (m, 3H), 6.97 (dd, J = 8.65, 8.81 Hz, 2H), 6.49 (d, J = 15.96 Hz, 1H), 3.63 ppm (s, 2H); ^{13}C NMR [150 MHz, DMSO-d_6]: δ = 173.7 (C), 165.5 (C), 152.0 (C), 147.0 (CH), 133.9 (C), 130.9 (C), 129.0 (CH), 128.9 (CH), 128.7 (CH), 128.3 (CH), 127.9 (CH), 123.9 (C), 122.0 (CH), 118.5 (CH), 116.7 (CH), 111.3 (CH), 33.3 ppm (CH_2); IR (KBr): ν_{max} = 3059, 3026, 1825, 1708, 1478, 1307, 1261, 1233, 1149, 1067, 920, 879, 866, 801, 765, 738, 709, 686 cm^{-1}. Compound purity (HPLC): 97.3%.

4.2.15. (E)-3-Chlorocinnamic acid 2-oxo-2,3-dihydro-benzofuran-5-yl ester (**8d**)

Yield: 367 mg (35%); R_f = 0.62 (ethyl acetate/petroleum ether (1:1)); mp: 85–95 °C ^{1}H NMR [600 MHz, DMSO-d_6]: δ = 7.77 (d, J = 15.99 Hz, 1H), 7.56–7.53 (m, 2H), 7.43–7.27 (m, 3H), 7.60 (dd, J = 8.89, 8.60 Hz, 2H), 6.60 (d, J = 16.00 Hz, 1H), 3.75 ppm (s, 2H); ^{13}C NMR [150 MHz, DMSO-d_6]: δ = 173.7 (C), 165.1 (C), 152.1 (C), 146.9 (C), 145.4 (CH), 135.7 (C), 135.0 (C), 130.7 (CH), 130.3 (CH), 127.6 (CH), 127.1 (CH), 126.0 (CH), 124.0 (C), 122.0 (CH), 118.5 (CH), 111.4 (CH), 33.3 ppm (CH_2); IR (KBr): ν_{max} = 3247, 3053, 1745, 1706, 1479, 1259, 1233, 1201, 1082, 1045, 893, 860, 842, 787, 753, 715, 688, 674 cm^{-1}. Compound purity (HPLC): 90.4%.

4.3. MAO activity measurements and inhibition

Human recombinant MAO-A and -B, expressed in baculovirus infected BTI insect cells, were used to evaluate the indole (**6a–h**) and benzofuran (**8a–d**) derivatives as potential MAO inhibitors. Both enzymes were purchased from Sigma–Aldrich® and stored at −70 °C until use. All incubations were performed in potassium phosphate buffer (100 mM, pH 7.4, made isotonic with KCl) and contained kynuramine (45 μM and 30 μM for MAO-A and -B, respectively), the enzyme (0.075 mg protein/mL), and various concentrations of the test inhibitors, producing a final incubation volume of 500 μL. Stock solutions of the test inhibitors were prepared in dimethyl sulfoxide (DMSO) and added to the incubation mixtures to yield a final DMSO concentration of 4% (v/v). DMSO concentrations higher than 4% are reported to inhibit MAO activity [40]. Samples were incubated at 37 °C for 20 min and the enzyme reactions were terminated by the addition of 200 μL sodium hydroxide (2 N) and centrifuged at 16,000*g* for 10 min. The supernatant fractions were removed and the concentrations of the MAO generated product, 4-hydroxyquinoline, were measured spectrofluorometrically at an excitation wavelength of 310 nm and an emission wavelength of 400 nm using a Varian® Cary Eclipse® fluorescence spectrophotometer. The IC_{50} values were determined from plots of the rate of MAO-A or -B catalysed 4-hydroxyquinoline formation versus the logarithm of the inhibitor concentration. For this purpose the Prism® 4.02 (GraphPad, Sorrento Valley, CA) software package was employed. Ten different concentrations of the test inhibitor, spanning three orders of magnitude were used to construct the sigmoidal dose–response curve. The IC_{50} values are reported as mean ± standard error of the mean (SEM) of duplicate determinations [29].

4.4. Time-dependent inhibition studies

Recombinant human MAO-B (0.03 mg protein/mL) was pre-incubated with **6g** (0.12 μM; 2 × IC_{50}) or **8b** (1.98 μM; 2 × IC_{50}) for periods of 0, 15, 30 and 60 min. These pre-incubations were carried out at 37 °C in potassium phosphate buffer (100 mM, pH 7.4, made isotonic with KCl). Kynuramine (30 μM) was added to the pre-incubations and the reactions were incubated for an additional 15 min at 37 °C. The reactions were terminated with the addition of sodium hydroxide (2 N) and the rates of 4-hydroxyquinoline formation were measured as described above. The final enzyme concentration in the incubations was 0.015 mg protein/mL and the final concentrations of **6g** and **8b** were 0.06 μM and 0.99 μM, respectively [41].

4.5. Examining the mode of inhibition

In order to determine the modes of inhibition of **6g**, Lineweaver–Burk plots were constructed by measuring the initial rates of MAO-B catalysed oxidation at four different kynuramine concentrations (15–90 μM) in the absence as well as in the presence of three different concentrations of the inhibitor. The concentration range chosen for **6g** was 0.015–0.06 μM. The reaction conditions and rate measurements were carried out as described above. Linear regression analysis was performed using the SigmaPlot software package (Systat Software Inc.).

4.6. Ligand docking

Manipulation of the crystal structure of MAO-B (PDB code: 2V5Z) [35] was performed with Discovery Studio® 1.7 (Accelrys Software Inc., San Diego, CA). The valences of the co-crystallised ligand (safinamide) and FAD co-factor were firstly corrected and hydrogen atoms were added. The receptor proteins were then typed by applying the CHARMm forcefield and a three-step minimisation protocol (steepest descent, conjugate gradient and adopted basis Newton-Rapheson) was performed while the protein backbone was kept rigid. During the minimisation cascade the Generalised Born with Simple Switching implicit solvation model was used to account for the effects of the aqueous environment. Minimisation of the receptor proteins were considered necessary since the protein X-ray structure might contain residual energetic tensions from the crystallisation process. Safinamide was subsequently eliminated from the energy-minimised receptor proteins and the backbone constraints were removed. The following conserved active site waters were retained: HOH 1155, 1169, 1346, 1351 (MAO-B, A-chain). The final modified proteins were used as the starting models for the docking simulation in Discovery Studio®. The structures of **6g** and **8d**, built and geometry optimised within Discovery Studio®, were docked into the protein model with LigandFit. Following the docking, the orientations and conformations of the docked ligands were further refined with the Smart Minimizer algorithm. All the parameters for the docking run were set to their default values. A total of ten docking solutions were allowed and the top-ranked docking conformations were determined using the DockScore values.

Acknowledgements

Financial support received from the National Research Foundation (South Africa) is gratefully acknowledged.

Appendix. Supplementary data

Supplementary data associated with this article can be found in the on-line version, at doi:10.1016/j.ejmech.2010.07.005.

References

[1] W. Dauer, S. Przedborski, Neuron 39 (2003) 889–909.
[2] D.A. Di Monte, L.E. De Lanney, I. Irwin, Brain Res. 738 (1996) 53–59.
[3] J. Saura, Z. Bleuel, J. Ulrich, A. Mendelowitsch, K. Chen, J.C. Shih, P. Malherbe, M. Da Prada, J.G. Richards, Neuroscience 70 (1996) 755–774.
[4] C.J. Fowler, A. Wiberg, L. Oreland, J. Marcusson, B. Winblad, J. Neural Transm. Gen. Sect. 49 (1980) 1–20.
[5] K.N. Westlund, R.M. Denney, R.M. Rose, C.W. Abell, Neuroscience 25 (1988) 439–456.
[6] A. Parkinson, B.W. Ogilvie, Biotransformation of xenobiotics. in: C.D. Klaassen (Ed.), Casarett & Doull's Toxicology: The Basic Science of Poisons. McGraw-Hill Inc., New York, 2008, pp. 204–206.
[7] G. Cohen, J. Neural Transm. Suppl. 32 (1990) 229–238.
[8] J. Knoll, K. Magyar, Adv. Biochem. Psychopharmcol. 5 (1972) 393–408.
[9] R.E. Heikkila, L. Manzino, F.S. Cabbat, R.C. Duvoisin, Nature 311 (1984) 467–469.
[10] P.H. Yu, B.A. Davis, D.A. Durden, A. Barber, I. Terleckyj, W.G. Nicklas, A.A. Boulton, J. Neurochem. 62 (1994) 697–704.
[11] C.W. Olanow, Ann. Neurol. Suppl. 32 (1992) S2–S9.
[12] J.P.M. Finberg, M. Tenne, M.B.H. Youdim, Br. J. Pharmacol. 73 (1981) 65–74.
[13] M.B.H. Youdim, A. Gross, J.P.M. Finberg, Br. J. Pharmacol. 132 (2001) 500–506.
[14] M.B.H. Youdim, W. Maruyama, M. Naoi, Drugs of Today 41 (2005) 369–391.
[15] K.F. Tipton, S. Boyce, J. O'Sullivan, G.P. Davey, J. Healy, Curr. Med. Chem. 11 (2004) 1965–1982.
[16] J.S. Fowler, N.D. Volkow, J. Logan, G.J. Wang, R.R. MacGregor, D. Schyler, A.P. Wolf, N. Pappas, D. Alexoff, C. Shea, Synapse 18 (1994) 86–93.
[17] F. Ooms, R. Frédérick, F. Durant, J.P. Petzer, N. Castagnoli Jr., C.J. Van der Schyf, J. Wouters, Bioorg. Med. Chem. Lett. 13 (2003) 69–73.
[18] F. Stocchi, L. Vacca, P. Grassini, M.F. De Pandis, G. Battaglia, C. Cattaneo, R.G. Fariello, Neurology 67 (2006) S24–S29.
[19] M.J. Matos, D. Viña, C. Picciau, F. Orallo, L. Santana, E. Uriarte, Bioorg. Med. Chem. Lett. 19 (2009) 5053–5055.
[20] D. Balsa, E. Fernández-Álvarez, K.F. Tipton, M. Unzeta, J. Neural Transm. Suppl. 32 (1990) 103–105.
[21] D. Balsa, E. Fernández-Álvarez, K.F. Tipton, M. Unzeta, Biochem. Soc. Trans. 19 (1991) 215–218.
[22] C. Fernández García, J.L. Marco, E. Fernández-Álvarez, Eur. J. Med. Chem. 27 (1992) 909–918.
[23] J.A. Morón, M. Campillo, V. Pérez, M. Unzeta, L. Pardo, J. Med. Chem. 43 (2000) 1684–1691.
[24] V. Pérez, J.L. Marco, E. Fernández-Álvarez, M. Unzeta, Br. J. Pharmacol. 127 (1999) 869–876.
[25] C.E. Müller, J. Sandoval-Ramírez, U. Schobert, U. Geis, W. Frobenius, K.-N. Klotz, Bioorg. Med. Chem. 6 (1998) 707–719.
[26] D. van den Berg, K.R. Zoellner, M.O. Ogunrombi, S.F. Malan, G. Terre'Blanche, N. Castagnoli Jr., J.J. Bergh, J.P. Petzer, Bioorg. Med. Chem. 15 (2007) 3692–3702.
[27] F. Suzuki, J. Shimada, S. Shiozaki, S. Ichikawa, A. Ishii, J. Nakamura, H. Nonaka, H. Kobayashi, E. Fuse, J. Med. Chem. 36 (1993) 2508–2518.
[28] E.F.V. Scriven, Chem. Soc. Rev. 12 (1983) 129–161.
[29] L. Novaroli, M. Reist, E. Favre, A. Carotti, M. Catto, P.-A. Carrupt, Bioorg. Med. Chem. 13 (2005) 6212–6217.
[30] Y.C. Cheng, W.H. Prusoff, Biochem. Pharmacol. 22 (1973) 3099–3108.
[31] R.R. Ramsay, C. Dunford, P.K. Gillman, Br. J. Pharmacol. 152 (2007) 946–951.
[32] P.K. Gillman, Can. J. Anaesth. 55 (2008) 311–312.
[33] J. Wouters, F. Ooms, S. Jegham, J. Koenig, P. George, F. Durant, Eur. J. Med. Chem. 32 (1997) 721–730.
[34] U. Thull, S. Kneubühler, P. Gaillard, P.-A. Carrupt, B. Testa, C. Altomare, A. Carotti, P. Jenner, K.St.P. McNaught, Biochem. Pharmacol. 50 (1995) 869–877.
[35] C. Binda, J. Wang, L. Pisani, C. Caccia, A. Carotti, P. Salvati, D.E. Edmondson, A. Mattevi, J. Med. Chem. 50 (2007) 5848–5852.
[36] J. Boström, J.R. Greenwood, J. Gottfries, J. Mol. Graph. Model. 21 (2003) 449–462.
[37] F. Chimenti, R. Fioravanti, A. Bolasco, P. Chimenti, D. Secci, F. Rossi, M. Yanez, F. Orallo, F. Ortuso, S. Alcaro, J. Med. Chem. 52 (2009) 2818–2824.
[38] S.-Y. Son, J. Ma, Y. Kondou, M. Yoshimura, E. Yamashita, T. Tsukihara, Proc. Natl. Acad. Sci. U S A 105 (2008) 5739–5744.
[39] A.P. Terent'ev, M.N. Preobrazhenskaya, A.S. Bebkov, G.M. Sorokina, Zh. Obshch. Khim. 29 (1959) 2541–2551;
Chem. Abstr. 54 (1960) 10991.
[40] C. Gnerre, M. Catto, F. Leonetti, P. Weber, P.-A. Carrupt, C. Altomare, A. Carotti, B. Testa, J. Med. Chem. 43 (2000) 4747–4758.
[41] H. Inoue, K. Castagnoli, C.J. van der Schyf, S. Mabic, K. Igarashi, N. Castagnoli Jr., J. Pharmacol. Exp. Ther. 291 (1999) 856–864.